

FDeID-Toolbox: Face De-Identification Toolbox

Hui Wei, Hao Yu, and Guoying Zhao

ELLIS Institute Finland
Center for Machine Vision and Signal Analysis (CMVS),
University of Oulu, Finland

Abstract. Face de-identification (FDeID) aims to remove personally identifiable information from facial images while preserving task-relevant utility attributes such as age, gender, and expression. It is critical for privacy-preserving computer vision, yet the field suffers from fragmented implementations, inconsistent evaluation protocols, and incomparable results across studies. These challenges stem from the inherent complexity of the task: FDeID spans multiple downstream applications (*e.g.*, age estimation, gender recognition, expression analysis) and requires evaluation across three dimensions (*e.g.*, privacy protection, utility preservation, and visual quality), making existing codebases difficult to use and extend. To address these issues, we present **FDeID-Toolbox**, a comprehensive toolbox designed for reproducible FDeID research. Our toolbox features a modular architecture comprising four core components: (1) standardized data loaders for mainstream benchmark datasets, (2) unified method implementations spanning classical approaches to SOTA generative models, (3) flexible inference pipelines, and (4) systematic evaluation protocols covering privacy, utility, and quality metrics. Through experiments, we demonstrate that **FDeID-Toolbox** enables fair and reproducible comparison of diverse FDeID methods under consistent conditions. The code is available at <https://github.com/infraface/FDeID-Toolbox>.

Keywords: Face De-Identification · Privacy Protection · Toolbox

1 Introduction

The proliferation of visual data collection from surveillance systems, social media platforms, and healthcare monitoring has intensified concerns about facial privacy [1]. Face de-identification (FDeID) addresses this issue by removing personally identifiable information from facial images while preserving task-relevant attributes such as age [2], gender [3], and expression [4]. This capability is essential for enabling privacy-preserving computer vision research and deployment, particularly as regulations like the EU AI Act (Regulation (EU) 2024/1689) [5] and HIPAA [6] impose strict requirements on biometric data processing.

Over the past two decades, the FDeID field has witnessed remarkable methodological diversity [7,8,9,10,11]. Early approaches relied on simple image processing

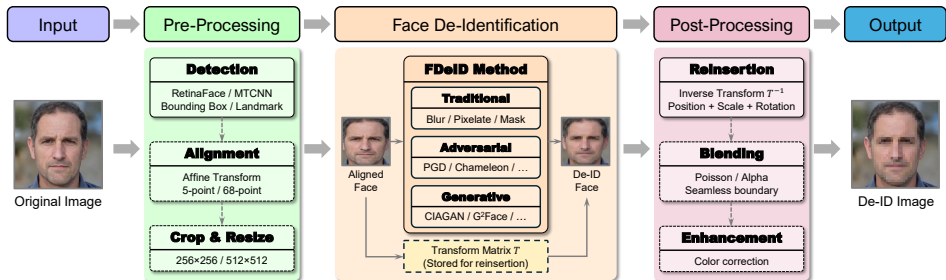


Fig. 1: FDeID Pipeline. An example of the components of a FDeID pipeline including pre-processing, face de-identification, and post-processing. Components shown with dashed borders are optional and method-dependent.

techniques such as blurring and pixelation [12,13], which provide intuitive privacy protection but severely degrade visual utility. Classical methods like k -Same [7] introduced principled privacy guarantees through k -anonymity [14], yet struggled with naturalness. More recently, adversarial perturbation-based methods [15,16] have emerged as a promising direction, crafting imperceptible noise to fool recognition systems while maintaining visual fidelity. In parallel, generative approaches leveraging GANs [17] and diffusion models [18] have advanced the realism of synthesized faces for FDeID. Across these diverse approaches, most FDeID methods share a common processing pipeline consisting of three stages, as shown in Figure 1: (i) optional pre-processing (*e.g.*, face detection, alignment, and cropping); (ii) the FDeID operation; and (iii) optional post-processing (*e.g.*, reinsertion, blending, and enhancement). The pre- and post-processing steps are method-dependent and not universally required.

Despite this methodological progress, the field suffers from standardization challenges that hinders scientific progress. Based on our review of literature in the field, we identified three factors that fragment the field and limit the interpretability and reproducibility of reported results. **First**, utility evaluation vary dramatically across existing FDeID methods [19,20,21,22]. For example, methods for human-computer interaction emphasize expression recognition [23,24], healthcare-oriented approaches require preservation of physiological signals such as remote photoplethysmography (rPPG) [25], and social media applications depend on demographic attributes (*e.g.*, age and gender) for content moderation [3,26]. The absence of a unified framework capable of evaluating multiple utility dimensions simultaneously makes it difficult to assess trade-offs between privacy protection and utility preservation. **Second**, evaluation protocols differ widely across studies, with inconsistent choices of datasets, recognition models, and metrics, rendering cross-method comparisons unreliable [27,28]. **Third**, existing implementations are scattered across heterogeneous and incompatible codebases, forcing researchers to re-implement methods and evaluation pipelines before conducting comparative studies, thereby impeding cumulative progress.

Table 1: Comparison of FDeID Toolboxes. Existing tools focus on specific method families and lack comprehensive utility evaluation, while our FDeID-Toolbox provides unified infrastructure spanning various method paradigms.

Toolbox	Dataset Support	Training Support	Utility Preservation Evaluation					
			Age	Gender	Ethnicity	Landmark	Expression	rPPG
DeepPrivacy [10]	✓	✓	✗	✗	✗	✗	✗	✗
DeepPrivacy2 [29]	✓	✓	✗	✗	✗	✗	✗	✗
deface [30]	✗	✗	✗	✗	✗	✗	✗	✗
FDeID-Toolbox (Ours)	✓	✓	✓	✓	✓	✓	✓	✓

Existing toolboxes (Table 1) address these issues only partially. DeepPrivacy [10] and DeepPrivacy2 [29] provide training for their own generative methods but support no other paradigms and evaluate no downstream utility. The lightweight deface [30] tool targets video anonymization via traditional methods alone, providing neither training nor evaluation. None of these tools implements a unified interface across method paradigms, supports more than one dataset, or evaluates more than a single downstream task.

To address these challenges, we introduce **FDeID-Toolbox**, a comprehensive toolbox designed as shared infrastructure for reproducible FDeID research. **FDeID-Toolbox** adopts a modular architecture with four core components: standardized data loaders for widely used benchmark datasets; unified implementations of representative FDeID methods spanning classical techniques, adversarial perturbations, and state-of-the-art generative models; flexible inference pipelines; and systematic evaluation protocols covering privacy protection, utility preservation, and visual quality. In total, the toolbox includes 17 representative FDeID methods exposed through a consistent `BaseDeidentifier` (see Algorithm 1) interface and supports extensible data loaders with standardized preprocessing. Evaluation is performed across privacy metrics, utility measures for six attributes (age, gender, ethnicity, landmarks, expression, and rPPG), and visual quality indicators, enabling fair and comprehensive comparison. All experiments are configured through YAML files, ensuring transparency and reproducibility. Together, these features position **FDeID-Toolbox** as a unified platform for rigorous, reproducible, and extensible research in FDeID.

2 Related Work

2.1 Face De-Identification

FDeID aims to remove personally identifiable information from facial images while preserving task-relevant attributes. Early approaches employed handcrafted image processing operations such as Gaussian blur, pixelation, and masking [12,13], which provide intuitive privacy protection but suffer from fundamental trade-offs between privacy and utility preservation. Formal privacy guarantees were introduced through k -anonymity [14] based methods: the k -Same algorithm [7] clusters faces and replaces each with the cluster average, theoretically bounding recognition accuracy at

$1/k$, with subsequent refinements addressing utility preservation [31,8,32]. Adversarial perturbation-based methods craft imperceptible noise to mislead face recognition systems [33,34,16], achieving near-perfect visual fidelity but facing transferability challenges across black-box settings. More recently, generative model-based approaches have emerged as the dominant paradigm: GAN-based methods [17,20,35] synthesize photorealistic de-identified faces through encoder-decoder architectures with identity-adversarial losses, while diffusion-based methods [27,18] achieve superior visual quality through iterative denoising. Specialized variants address reversibility for authorized recovery [21,36], attribute preservation [24,37], and domain-specific utility requirements such as rPPG signal preservation [25]. Despite this methodological richness, the field suffers from fragmented implementations across incompatible codebases, inconsistent evaluation metrics, and narrow utility assessments. These challenges motivate the development of the **FDeID-Toolbox**.

Algorithm 1 Base De-identifier Interface

```
# All methods inherit from BaseDeidentifier
class BaseDeidentifier:
    def __init__(self, config):
        self.config = config
        self.device = config.get("device", "cuda")

    def deidentify(self, face_img):
        """Apply de-identification to aligned face."""
        raise NotImplementedError

# Example usage
config = {"method": "CIAGAN", "device": "cuda"}
deid = BaseDeidentifier(config)
result = deid.deidentify(aligned_face) # [H, W, C]
```

2.2 Existing Tools

As shown in Table 1, several open-source tools have been developed for the FDeID task, yet each addresses only a narrow subset of research requirements. DeepPrivacy [10] pioneered GAN-based FDeID with a conditional inpainting approach, later extended in DeepPrivacy2 [29] to support full-body de-identification at higher resolution. While these tools provide training infrastructure for their specific generative methods, they lack multiple dataset loaders and do not evaluate utility preservation across downstream tasks. The deface [30] tool offers a lightweight command-line interface for video anonymization using traditional methods (blur, pixelation, masking), but provides no training capability, evaluation framework, or support for learning-based methods. Critically, none of these tools support comprehensive evaluation across privacy, utility, and quality dimensions. Our **FDeID-Toolbox** addresses these limitations by unifying representative methods under a common interface, providing data loaders for mainstream datasets, and implementing systematic evaluations covering six utility attributes alongside privacy and quality metrics.

3 The FDeID-Toolbox

3.1 Architecture Overview

FDeID-Toolbox is built around three design principles that directly address the standardization gaps identified in Section 1. *Modularity*: each component exposes a well-defined interface so that datasets, methods, and metrics can be swapped or extended without touching other parts of the codebase. *Reproducibility*: every experiment is fully specified by a single YAML file covering dataset paths, method hyperparameters, model checkpoints, and evaluation criteria, making results shareable and auditable. *Comprehensiveness*: rather than optimizing for a single method family or evaluation dimension, the toolbox covers all three paradigms (traditional, adversarial, generative) and all three evaluation dimensions (privacy, utility, quality).

As shown in Figure 2, **FDeID-Toolbox** comprises four tightly integrated modules. The **Data Module** provides standardised data loaders and preprocessing pipelines for six benchmark datasets, exposing a common **BaseDataset** interface that supports custom datasets with minimal boilerplate. The **Method Module** implements 17 FDeID algorithms under a shared **BaseDeidentifier** interface (Algorithm 1), ensuring that every method can be invoked, benchmarked, and composed identically regardless of its underlying paradigm. The **Pipeline Module** orchestrates the complete FDeID workflow with each stage independently configurable and optional. The **Evaluation Module** unifies privacy, utility, and quality assessment into a single pass, computing all metrics from the same de-identified outputs under identical conditions.

3.2 Supported Datasets

Dataset selection is driven by coverage across the three evaluation dimensions and the six utility attributes. The data module currently supports the following datasets: 1) **CelebA-HQ** [38] contains 30,000 high-quality face images at 1024×1024 resolution, selected from CelebA [39] and annotated with 40 binary attributes (e.g., *Smiling*, *Eyeglasses*, *Young*). We specifically leverage it for landmark utility evaluation. 2) **LFW** [40] comprises 13,233 unconstrained face images of 5,749 identities collected from the web and is used for privacy and visual quality evaluation. 3) **AgeDB** [41] includes 16,516 in-the-wild face images of 570 identities with age annotations and is used for both privacy and age-related utility evaluation. 4) **FairFace** [42] consists of 108,501 images with balanced annotations for ethnicity, gender, and age, and is employed for utility evaluation of gender and ethnicity. 5) **AffectNet** [43] contains over one million facial images annotated with expression labels and is used for expression-related utility evaluation. 6) **PURE** [44] comprises recordings of 10 identities captured under six different setups, resulting in 60 one-minute video sequences, and is used for evaluating rPPG preservation.

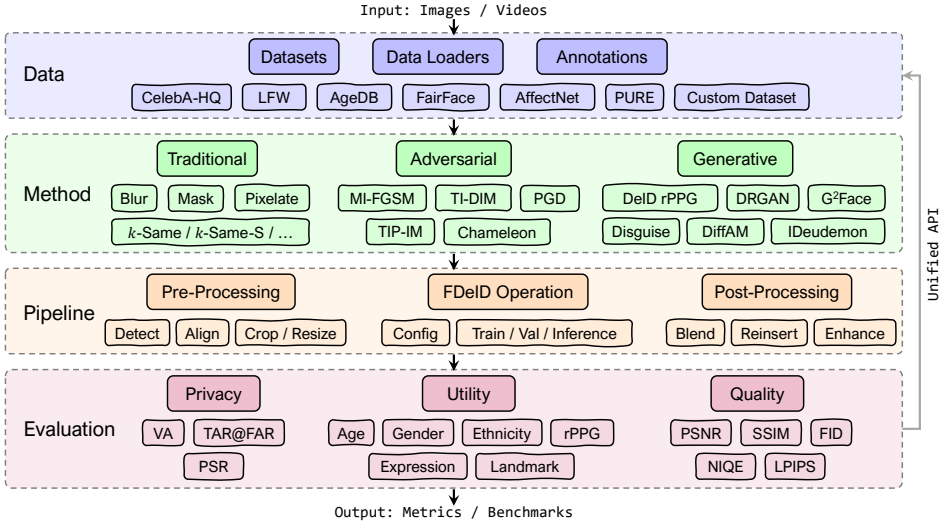


Fig. 2: Architecture of the **FDeID-Toolbox**. The modular design comprises four core modules: **Data** for unified dataset management, **Methods** spanning traditional, adversarial, and generative approaches, **Pipeline** for pre-processing, training, and post-processing, and **Evaluation** integrating privacy, utility, and quality metrics. Components communicate through a unified API, enabling plug-and-play extensibility.

3.3 Implemented Methods

FDeID-Toolbox implements 17 representative FDeID methods spanning three technical paradigms. *Traditional methods* achieve privacy through explicit visual degradation or face substitution without learned models. *Adversarial methods* craft imperceptible perturbations that fool face recognition systems while leaving the image visually intact. *Generative methods* synthesize a new facial appearance via learned generative models, offering the greatest flexibility in balancing privacy with visual realism.

Traditional Methods implement naive image processing techniques and the *k-Same* family, requiring no training. Naive methods include *Blur*, *Pixelation*, and *Mask*, which serve as important baselines and remain widely deployed in practice despite their limitations. The *k-Same* family replaces each face with a combination of its k nearest neighbors in embedding space: *k-Same* [7] substitutes a face with the pixel-wise mean of k neighbors; *k-Same-Select* [31] selects a single representative from the k candidates; and *k-Same-Furthest* [32] maximizes privacy by choosing the most dissimilar face within the k -neighbor set.

Adversarial Methods craft imperceptible perturbations to fool face recognition systems. Our toolbox includes *MI-FGSM* [15], *PGD* [45], *TI-DIM* [46], *TIP-IM* [16], and *Chameleon* [2]. These methods optimize adversarial perturbation δ to maximize recognition loss while constraining $\|\delta\|_\infty \leq \epsilon$.

Generative Methods synthesize de-identified face images using learned generative models. *CIAGAN* [20] employs a conditional GAN with an identity-guided

discriminator to generate de-identified faces. *Adv-Makeup* [47] transfers adversarial makeup patterns onto facial regions to mislead recognition systems while maintaining visually plausible appearances. *AMT-GAN* [48] extends adversarial makeup transfer by incorporating feature disentanglement to improve visual quality. *DeID-rPPG* [25] performs video-based FDeID while preserving rPPG signals for health monitoring. *G²Face* [36] enables high-fidelity, reversible face de-identification, allowing authorized re-identification when required. *WeakenDiff* [49] leverages diffusion models to adversarially modify latent representations for identity suppression.

3.4 Pre-Processing, FDeID Operation, and Post-Processing

FDeID-Toolbox provides end-to-end pipelines standardizing the complete FDeID workflow. As shown in Figure 1, the pipeline comprises three independently configurable stages; pre- and post-processing are optional and method-dependent.

Pre-Processing. For methods operating on cropped face regions, raw images are transformed into standardized inputs via three steps: (i) *face detection* using RetinaFace [50], yielding bounding boxes and facial landmarks; (ii) *alignment* via an affine transformation computed from the detected landmarks, with the transform matrix T stored for later reinsertion; and (iii) *cropping and resizing* to a standardized resolution.

FDeID Operation. All methods are configured via YAML files specifying hyperparameters, model paths, and evaluation settings. Traditional and adversarial methods require no training; generative methods implement a `BaseTrainer` interface supporting GAN-based and diffusion-based paradigms with checkpointing and loss logging. At inference, all methods expose a unified `BaseDeidentifier` interface dispatched via `get_deidentifier(config)`.

Post-Processing. For methods operating on cropped regions, the de-identified face is reintegrated into the original image via: (i) *reinsertion* using the inverse transform T^{-1} encoding position, scale, and rotation; (ii) *blending* to eliminate boundary artifacts; and (iii) optional *enhancement* to reconcile chromatic inconsistencies with the surrounding image.

4 Benchmarking and Analysis

4.1 Metrics

Following the mainstream methods [20,2], we evaluate FDeID methods across three dimensions: privacy, utility, and quality.

Privacy Metrics. We measure FDeID effectiveness using face verification accuracy on multiple recognition models and report: (1) *Verification Accuracy* (VA \downarrow): the rate at which de-identified faces are correctly matched to originals at a fixed threshold; (2) *True Accept Rate at 0.1% FAR* (TAR@FAR=0.1% \downarrow): verification rate under strict security settings; and (3) *Protection Success Rate* (PSR \uparrow): also

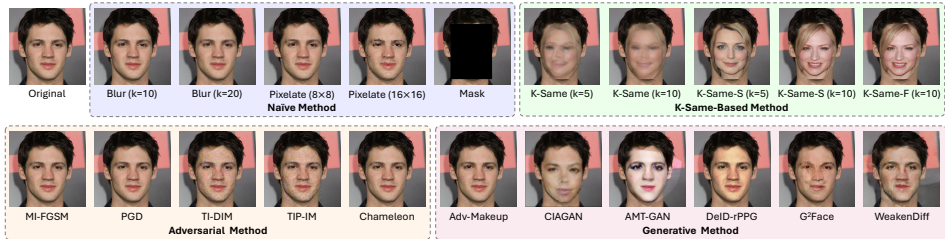


Fig. 3: **Qualitative comparison of FDeID methods on a sample face image.** Traditional naive methods (blur, pixelate, mask, k-Same variants [7,31,32]) provide privacy but degrade visual quality. Adversarial methods (MI-FGSM [15], PGD [45], TI-DIM [46], TIP-IM [16], Chameleon [2]) focus on introducing visually imperceptible perturbations. Generative methods (Adv-Makeup [47], CIAGAN [20], AMT-GAN [48], DeID-rPPG [25], G²Face [36], WeakenDiff [49]) synthesize de-identified faces with varying degrees of identity change and visual realism.

known as Attack Success Rate (ASR), percentage of faces successfully de-identified below the recognition threshold.

Utility Metrics. We assess utility preservation using pre-trained classifiers for age (Mean Absolute Error, MAE \downarrow), gender (Accuracy, Acc \uparrow), ethnicity (Accuracy, Acc \uparrow), expression (Accuracy, Acc \uparrow), and landmark detection (Normalized Mean Error, NME \downarrow). For rPPG preservation, we measure Mean Absolute Error of estimated heart rate (HR-MAE \downarrow).

Quality Metrics. Visual quality, in the context of FDeID, refers to the degree to which a de-identified image preserves the original image’s appearance (*e.g.*, pixel structure, perceptual texture, distribution) independent of identity. This source-fidelity framing is distinct from assessing whether a synthesized face looks photorealistic as a new identity. We evaluate source fidelity through five complementary metrics. *PSNR* \uparrow and *SSIM* \uparrow [51] measure pixel-level fidelity. *LPIPS* \downarrow [52] quantifies perceptual distance using deep features. *FID* \downarrow [53] assesses distributional similarity between de-identified and real face sets via Inception-v3 [54] features, capturing overall realism. *NIQE* \downarrow [55] provides reference-free quality assessment by measuring deviation from natural scene statistics.

4.2 Implementation Details

We use RetinaFace [50] with five-point landmarks for face detection and alignment. Age prediction is evaluated on AgeDB [41], while gender and ethnicity classification are conducted on FairFace [42] using 224×224 inputs, covering two gender classes and seven ethnicity categories. Expression recognition employs POSTER [56] with 224×224 inputs and seven expression classes. Facial landmark detection is performed using HRNet [57], which predicts 29 keypoints from 256×256 inputs. For rPPG preservation, we adopt FactorizePhys [58], a video-based model with 3D convolutional blocks and factorized self-attention based on non-negative matrix factorization, operating on video clips of 160 frames at a resolution of 72×72 . For

Table 2: **Privacy protection performance on LFW [40] and AgeDB [41].** We report verification accuracy (VA \downarrow), TAR@FAR=0.1% \downarrow , and Protection Success Rate (PSR \uparrow) across three recognition models (ArcFace [59], CosFace [60], AdaFace [61]). Darker background colors indicate better performance. All results are from our unified re-implementation under identical conditions.

Method	Type	LFW									AgeDB								
		ArcFace-R100			CosFace-R50			AdaFace-R50			ArcFace-R100			CosFace-R50			AdaFace-R50		
		VA \downarrow	TAR \downarrow	PSR \uparrow	VA \downarrow	TAR \downarrow	PSR \uparrow	VA \downarrow	TAR \downarrow	PSR \uparrow	VA \downarrow	TAR \downarrow	PSR \uparrow	VA \downarrow	TAR \downarrow	PSR \uparrow	VA \downarrow	TAR \downarrow	PSR \uparrow
Original (No Face De-ID)	-	99.25	98.37	-	99.23	98.33	-	99.23	98.40	-	98.17	95.82	-	98.05	95.62	-	97.71	93.57	-
Gaussian Blur ($\sigma=10$)	Naive	99.22	98.33	0.40	99.26	98.47	0.40	98.97	97.83	0.73	96.31	86.57	5.58	96.29	84.03	5.41	95.77	83.03	4.18
Gaussian Blur ($\sigma=20$)	Naive	98.23	93.50	3.37	98.25	94.60	2.53	97.37	84.80	3.27	91.14	48.63	22.57	91.50	57.65	20.19	89.84	30.81	16.97
Pixelation (8 \times 8)	Naive	78.11	4.07	29.35	80.45	3.24	38.36	74.06	0.45	42.25	82.43	4.11	45.79	84.38	2.54	39.73	84.28	28.38	32.88
Pixelation (16 \times 16)	Naive	60.29	1.45	21.74	63.97	4.35	10.14	61.03	1.45	8.70	93.33	0.00	27.27	80.00	0.00	27.27	86.67	0.00	9.09
Black Mask	Naive	83.33	42.86	57.14	83.33	57.14	35.71	83.33	28.57	57.14	59.29	0.30	6.60	56.15	0.43	0.03	57.27	0.63	9.94
k -Same ($k=5$)	Class.	65.58	3.50	70.73	67.72	3.37	56.80	65.97	2.87	51.93	56.87	0.93	76.65	57.60	0.87	65.91	57.20	0.50	49.87
k -Same ($k=10$)	Class.	68.52	3.47	54.53	70.34	4.40	37.37	67.74	4.17	33.63	57.35	0.73	64.81	58.05	1.13	47.63	57.34	1.33	30.89
k -Same-Select ($k=5$)	Class.	57.58	0.73	94.73	57.86	0.93	93.73	58.12	0.63	92.80	52.12	0.70	94.13	52.28	0.70	93.10	52.92	0.57	90.29
k -Same-Select ($k=10$)	Class.	57.20	0.40	95.57	58.40	0.60	94.63	57.72	0.30	93.30	52.10	0.33	94.86	52.95	0.43	93.96	51.53	0.40	91.53
k -Same-Furthest ($k=10$)	Class.	56.80	0.33	95.30	58.03	0.33	94.37	57.09	0.23	93.33	52.10	0.20	95.10	52.57	0.20	93.76	52.07	0.17	91.16
MI-FGSM [15] ($\epsilon=8$)	Adv.	95.77	80.13	16.47	98.09	94.17	5.80	98.71	96.47	1.90	94.53	82.52	12.55	95.38	85.42	6.87	95.53	82.12	4.47
PGD [45] ($\epsilon=8$)	Adv.	97.29	91.93	7.70	98.85	97.03	2.07	99.02	97.97	0.83	95.63	88.76	6.61	96.36	88.39	4.24	96.35	85.79	2.90
TI-DIM [46] ($\epsilon=8$)	Adv.	94.80	79.23	23.00	97.02	90.80	12.37	97.88	93.63	5.10	91.74	67.99	25.90	93.48	69.33	17.39	93.71	77.24	10.05
TIP-IM [16] ($\epsilon=8$)	Adv.	94.69	79.10	22.77	97.22	86.90	12.80	97.82	93.33	4.67	91.27	61.58	24.53	92.98	70.56	16.86	93.64	75.90	9.65
Chameleon [2] ($\epsilon=8$)	Adv.	97.68	91.53	6.63	99.06	97.97	1.53	99.18	98.10	0.40	96.20	89.89	5.94	96.68	88.73	3.30	96.62	89.26	2.13
Adv-Makeup [47]	Gen.	99.25	98.37	0.00	99.23	98.33	0.00	99.23	98.37	0.03	97.98	95.23	0.27	97.93	94.76	0.10	97.57	93.53	0.27
CIAGAN [20]	Gen.	74.82	7.33	59.83	75.85	6.40	52.20	73.18	7.73	46.93	60.95	2.27	77.08	61.79	2.10	68.25	62.35	2.03	55.34
AMT-GAN [48]	Gen.	99.29	82.70	3.90	95.85	77.77	2.50	95.15	70.80	2.13	93.53	60.74	5.97	92.01	54.17	4.14	90.81	46.80	3.97
DeID+rPPG [25]	Gen.	99.25	98.37	0.00	99.23	98.37	0.00	99.22	98.37	0.03	97.92	95.10	0.57	97.75	95.00	0.17	97.45	93.66	0.43
G ² Face [36]	Gen.	96.94	87.00	7.47	96.98	87.90	8.23	95.91	75.70	8.90	92.51	62.98	20.71	91.86	55.57	19.65	89.95	52.77	18.41
WeakenDiff [49]	Gen.	91.05	43.17	21.13	92.51	54.63	12.73	90.86	56.17	13.47	90.52	54.66	10.33	90.71	39.28	6.37	89.02	38.23	6.33

adversarial-based methods, we set the perturbation budget to $\epsilon=8/255$, the step size to $\alpha=2/255$, and the number of iterations to 20 under an ℓ_∞ norm constraint. All experiments are conducted on the supercomputer using AMD MI250X GPUs with ROCm 6.2.2 and PyTorch 2.5.1.

4.3 Benchmark Results

We conduct comprehensive benchmarking of 17 FDeID methods re-implemented within **FDeID-Toolbox**, evaluating privacy protection (Table 2), utility preservation (Table 3), and visual quality (Table 4). All methods are evaluated under identical conditions using our standardized pipelines and all reported numbers are produced by our own implementations. We do not report numbers taken directly from original papers, as differences in evaluation protocols, datasets, and recognition models across studies make such numbers incomparable.

Privacy Protection. Table 2 reveals substantial performance disparities across method paradigms. Classical k -anonymity methods, particularly k -Same-Select and k -Same-Furthest, achieve the strongest privacy protection with PSR exceeding 90% across all recognition models and datasets, while maintaining verification accuracy near chance level (\sim 50-58%). These methods effectively disrupt identity features by replacing faces with carefully selected alternatives from the k -neighbor set. In contrast, adversarial perturbation methods demonstrate limited effectiveness under our evaluation protocol: despite their theoretical foundation in fooling recognition systems, methods like PGD and Chameleon achieve PSR below 10% on LFW,

Table 3: **Utility preservation performance across six downstream tasks.** We evaluate age estimation (MAE \downarrow) on AgeDB [41], gender and ethnicity classification (Acc \uparrow) on FairFace [42], expression recognition (Acc \uparrow) on AffectNet [43], landmark detection (NME \downarrow) on CelebA-HQ [38], and rPPG estimation (HR-MAE \downarrow) on PURE [44]. All results are from our unified re-implementation under identical conditions.

Method	Type	Age	Gender	Ethnicity	Expression	Landmark	rPPG
		MAE \downarrow	Acc \uparrow	Acc \uparrow	Acc \uparrow	NME \downarrow	HR-MAE \downarrow
Original	–	10.18	94.39	71.99	70.54	0.3601	0.39
Gaussian Blur ($\sigma=10$)	Naive	12.00	93.97	71.35	54.09	0.3609	0.40
Gaussian Blur ($\sigma=20$)	Naive	14.18	93.55	69.33	24.56	0.3620	0.40
Pixelation (8×8)	Naive	15.26	90.48	59.76	14.79	0.3615	4.10
Pixelation (16×16)	Naive	18.93	70.40	17.12	15.55	0.3772	4.50
Black Mask	Naive	18.31	65.36	20.26	14.63	0.8733	17.56
k -Same ($k=5$)	Class.	15.91	70.74	27.30	18.01	0.3751	24.13
k -Same ($k=10$)	Class.	16.00	71.90	27.52	20.27	0.3802	23.40
k -Same-Select ($k=5$)	Class.	17.64	60.22	21.03	15.87	0.3923	31.11
k -Same-Select ($k=10$)	Class.	17.81	59.16	20.49	15.55	0.3973	32.56
k -Same-Furthest ($k=10$)	Class.	18.38	56.43	20.39	15.35	0.3974	28.37
MI-FGSM [15] ($\epsilon=8$)	Adv.	10.29	91.93	66.16	69.26	0.3601	1.70
PGD [45] ($\epsilon=8$)	Adv.	10.04	93.31	69.44	69.91	0.3599	1.65
TI-DIM [46] ($\epsilon=8$)	Adv.	10.91	88.91	61.05	68.70	0.3628	5.37
TIP-IM [16] ($\epsilon=8$)	Adv.	10.95	88.64	61.59	68.90	0.3630	3.60
Chameleon [2] ($\epsilon=8$)	Adv.	9.95	93.25	70.19	70.30	0.3599	1.96
Adv-Makeup [47]	Gen.	10.28	94.05	70.93	70.48	0.3613	0.40
CIAGAN [20]	Gen.	18.47	56.56	19.89	28.99	0.4242	9.01
AMT-GAN [48]	Gen.	16.95	92.46	64.53	66.28	0.3595	26.17
DeID-rPPG [25]	Gen.	10.78	94.03	70.28	69.38	0.3627	0.39
G ² Face [36]	Gen.	11.82	90.61	63.61	63.27	0.3629	20.16
WeakenDiff [49]	Gen.	11.46	86.63	55.24	65.36	0.3603	13.90

indicating that the perturbations optimized against surrogate models (ArcFace) fail to transfer reliably to unseen recognizers. Among generative methods, CIAGAN provides moderate privacy protection (PSR of 46-77% depending on the recognizer), while Adv-Makeup and DeID-rPPG show near-zero PSR, suggesting their modifications are insufficient to alter identity-discriminative features. Traditional naive methods exhibit inconsistent behavior: pixelation at 16×16 resolution achieves low verification accuracy but also low PSR due to complete facial structure destruction, whereas Gaussian blur preserves too much identity information even at $\sigma=20$. These findings highlight that effective privacy protection requires explicit identity feature manipulation rather than generic image degradation or imperceptible perturbations.

Utility Preservation. Table 3 demonstrates the inherent trade-off between privacy protection and utility preservation across FDeID methods. Adversarial perturbation methods excel at utility preservation, with Chameleon and PGD maintaining near-original performance across all six attributes (age MAE of 9.95-10.04 *vs.* original 10.18; expression accuracy of 69.91-70.30% *vs.* original 70.54%). This is expected since these methods introduce only minimal, imperceptible modifications to the input images. Generative methods exhibit mixed utility profiles: DeID-rPPG preserves rPPG signals exceptionally well (HR-MAE of 0.39, identical to original)

Table 4: **Visual quality assessment on LFW [40] and AgeDB [41].** PSNR \uparrow and SSIM \uparrow measure pixel-level fidelity; FID \downarrow and NIQE \downarrow assess perceptual realism; LPIPS \downarrow quantifies perceptual distance. All results are from our unified re-implementation.

Method	Type	LFW					AgeDB				
		PSNR \uparrow	SSIM \uparrow	FID \downarrow	NIQE \downarrow	LPIPS \downarrow	PSNR \uparrow	SSIM \uparrow	FID \downarrow	NIQE \downarrow	LPIPS \downarrow
Gaussian Blur ($\sigma=10$)	Naive	35.90	0.9657	4.28	7.7854	0.0470	31.02	0.8957	12.81	9.5337	0.1515
Gaussian Blur ($\sigma=20$)	Naive	31.89	0.9339	11.81	8.4497	0.1033	27.82	0.8353	31.82	11.1360	0.2447
Pixelation (8 \times 8)	Naive	28.13	0.8862	43.43	6.4532	0.2091	24.22	0.7441	101.97	7.1216	0.3970
Pixelation (16 \times 16)	Naive	24.52	0.8555	55.47	7.5537	0.2193	20.90	0.6846	133.82	9.5578	0.4159
Black Mask	Naive	12.64	0.7500	101.92	9.3674	0.2474	8.67	0.4542	179.04	16.0312	0.4637
k -Same ($k=5$)	Class.	26.15	0.9000	7.19	5.6633	0.0878	21.20	0.7742	27.46	5.3888	0.2162
k -Same ($k=10$)	Class.	26.28	0.9029	9.44	6.0672	0.0884	21.34	0.7815	32.33	5.8310	0.2175
k -Same-Select ($k=5$)	Class.	24.26	0.8823	4.97	5.2572	0.0988	19.23	0.7382	14.42	5.3431	0.2334
k -Same-Select ($k=10$)	Class.	24.04	0.8808	4.96	5.2356	0.1000	18.99	0.7350	14.77	5.3041	0.2366
k -Same-Furthest ($k=10$)	Class.	23.72	0.8786	5.06	5.1978	0.1015	18.63	0.7304	15.53	5.2617	0.2411
MI-FGSM [15] ($\epsilon=8$)	Adv.	37.78	0.9561	12.22	4.5203	0.0768	34.81	0.9165	21.25	4.3010	0.1503
PGD [45] ($\epsilon=8$)	Adv.	40.21	0.9720	5.98	4.6529	0.0529	37.16	0.9466	11.86	4.4361	0.1100
TI-DIM [46] ($\epsilon=8$)	Adv.	37.65	0.9744	5.32	5.0848	0.0500	34.32	0.9517	18.64	4.7763	0.1259
TIP-IM [16] ($\epsilon=8$)	Adv.	37.68	0.9744	5.39	5.0823	0.0500	34.35	0.9517	18.61	4.7778	0.1256
Chameleon [2] ($\epsilon=8$)	Adv.	41.28	0.9809	4.40	4.6381	0.0418	38.21	0.9656	11.59	4.6091	0.0895
Adv-Makeup [47]	Gen.	46.53	0.9961	0.13	5.5207	0.0049	41.49	0.9937	1.60	5.2059	0.0120
CIAGAN [20]	Gen.	25.71	0.9065	4.12	6.9326	0.0825	19.58	0.7349	43.84	8.1664	0.2884
AMT-GAN [48]	Gen.	25.73	0.9383	5.62	5.2237	0.0837	25.89	0.9422	12.73	5.2373	0.0837
DeID-rPPG [25]	Gen.	35.71	0.9893	0.84	5.7132	0.0218	28.59	0.9478	9.10	6.0071	0.1245
G ² Face [36]	Gen.	32.32	0.9676	2.51	5.3526	0.0352	28.05	0.9252	14.22	5.0341	0.1015
WeakenDiff [49]	Gen.	28.84	0.8700	9.08	5.9011	0.1563	27.48	0.8179	9.61	5.5688	0.2030

and maintains strong demographic attribute accuracy, while Adv-Makeup achieves similar preservation due to its localized makeup-region modifications. However, CIAGAN suffers severe utility degradation across all attributes (gender accuracy drops to 56.56%, expression to 28.99%), reflecting its aggressive face replacement strategy. The k -Same family methods show consistently poor utility preservation, with k -Same-Furthest exhibiting the worst performance (age MAE of 18.38, gender accuracy of 56.43%, rPPG HR-MAE of 28.37), as maximizing identity dissimilarity inherently disrupts attribute-correlated features. Naive methods demonstrate attribute-dependent degradation: Gaussian blur preserves demographic attributes reasonably well but severely impacts expression recognition (24.56% at $\sigma=20$), while black masking catastrophically fails for landmark detection (NME of 0.8733) and rPPG estimation (HR-MAE of 17.56). These results underscore the importance of multi-attribute utility evaluation, as methods optimized for specific downstream tasks may fail unexpectedly on others.

Visual Quality. Table 4 reveals that different metrics capture complementary aspects of visual quality, and single-metric evaluation can be misleading. Adv-Makeup achieves the highest pixel-level and perceptual fidelity across the board because it restricts modifications to the makeup region, leaving the remaining facial structure intact. DeID-rPPG similarly attains high structural fidelity (PSNR of 35.71 dB, FID of 0.84) through its subtle temporal adjustments. Among adversarial methods, Chameleon achieves the best balance (PSNR of 41.28 dB, FID of 4.40, NIQE of 4.64), while MI-FGSM attains a comparable PSNR but incurs a much higher FID, indicating that its structured gradient-aligned noise introduces feature-

level distributional shifts not captured by pixel metrics alone. A concrete example of inter-metric disagreement also seen in AMT-GAN, which achieves only moderate PSNR yet competitive FID because its synthesis produces perceptually realistic outputs. A notable cross-dataset finding is that CIAGAN’s FID deteriorates sharply from 4.12 on LFW to 43.84 on AgeDB, exposing distributional fragility beyond its training domain. k -Same methods yield moderate fidelity but competitive NIQE scores, since they substitute real face images whose natural texture statistics are well-preserved; black masking, by contrast, yields the worst results across all metrics. Counterintuitively, adversarial methods achieve the best NIQE scores (4.52–5.08) among all paradigms, outperforming even generative methods (5.22–6.93), because their perturbations are constrained to a tight ℓ_∞ ball that preserves low-level natural image statistics. Collectively, these results confirm a general inverse relationship between privacy protection and visual quality, and underscore the necessity of multi-metric evaluation for reliable quality assessment in FDeID.

4.4 Privacy-Utility-Quality Trade-off Analysis

Jointly analyzing Table 2–Table 4, methods cluster into distinct operating regimes. At one extreme, adversarial methods (PGD, Chameleon) and localized generative methods (Adv-Makeup, DeID-rPPG) achieve near-original utility and excellent visual quality but provide negligible privacy protection (PSR < 4%), as perturbations optimized against surrogate recognizers fail to transfer reliably to unseen models. At the opposite extreme, k -Same-Select and k -Same-Furthest deliver robust privacy (PSR > 93%) at the cost of severe utility degradation (gender accuracy falling to 56–60%, rPPG HR-MAE deteriorating from 0.39 to >28) and moderate quality reduction (PSNR of 23–24 dB). Between these extremes, CIAGAN achieves moderate privacy but occupies an unfavorable position: it simultaneously incurs severe utility loss (gender accuracy of 56.56%, expression of 28.99%) and cross-domain quality fragility (FID rising from 4.12 on LFW to 43.84 on AgeDB), offering no compelling advantage over either regime. More nuanced attribute-level trade-offs emerge in other methods: G²Face achieves good visual quality (PSNR of 32.32 dB, FID of 2.51) yet its rPPG utility degrades substantially (HR-MAE of 20.16), showing that strong appearance fidelity does not guarantee preservation of physiological signals; AMT-GAN preserves facial landmarks best of all methods (NME of 0.3595) and maintains high gender accuracy (92.46%), yet exhibits the worst rPPG among generative methods (HR-MAE of 26.17), underscoring that utility preservation is highly attribute-specific.

These observations reveal two patterns: utility and visual quality are *positively correlated*, since both benefit from minimal image modification, while both exhibit *negative correlations* with privacy protection effectiveness. Crucially, no evaluated method simultaneously achieves strong privacy (PSR > 90%), high utility (< 2% relative degradation across all attributes), and excellent visual quality (PSNR > 35 dB), confirming an open research challenge: developing FDeID techniques that can selectively suppress identity-discriminative features while preserving the full set

Table 5: **Method ensemble results.** Different ensemble strategies achieve varied privacy-utility-quality trade-offs. VA, TAR, and PSR are averaged across three recognizers (ArcFace [59], CosFace [60], AdaFace [61]). Best results are highlighted in bold.

Ensemble Type	Configuration	Privacy			Utility				Quality
		VA↓	TAR↓	PSR↑	Age↓	Gender↑	Expr↑	rPPG↓	PSNR↑
<i>Single Methods (Baselines)</i>									
–	CIAGAN	74.62	7.15	52.99	18.47	56.56	28.99	9.01	25.71
–	TI-DIM ($\epsilon=8$)	96.57	87.89	13.49	10.91	88.91	68.70	5.37	37.65
–	k -Same-Select ($k=5$)	57.85	0.76	93.75	17.64	60.22	15.87	31.11	24.26
–	DeID-rPPG	99.23	98.37	0.01	10.78	94.03	69.38	0.39	35.71
<i>Sequential Ensemble</i>									
Sequential	CIAGAN → TI-DIM	68.46	3.00	77.75	12.57	56.74	27.62	22.91	25.02
Sequential	k -Same-Select → TI-DIM	86.96	43.54	46.99	12.57	87.79	36.57	4.07	33.69
Sequential	DeID-rPPG → CIAGAN	73.69	5.18	54.94	18.95	54.90	28.76	7.55	24.34
<i>Parallel Ensemble (Weighted Fusion)</i>									
Parallel	$0.7 \times \text{CIAGAN} + 0.3 \times k\text{-Same-Select}$	77.70	8.72	46.42	17.32	65.62	31.77	8.52	27.77
Parallel	$0.5 \times \text{CIAGAN} + 0.5 \times \text{DeID-rPPG}$	96.17	85.38	8.67	13.14	82.75	59.71	7.01	30.85
Parallel	$0.6 \times k\text{-Same-Select} + 0.4 \times \text{TI-DIM}$	98.99	97.82	0.71	11.09	93.49	68.29	1.59	38.82
<i>Attribute-Guided Ensemble</i>									
Attr-Guided	preserve={gender, expr}, suppress={identity}	96.99	89.85	10.42	10.75	89.47	69.20	2.38	38.17
Attr-Guided	preserve={age, rPPG}, suppress={identity, ethnicity}	97.04	90.27	10.43	10.76	89.47	69.42	4.48	38.18
Attr-Guided	preserve={landmark}, suppress={identity, gender}	96.96	89.41	10.84	10.75	89.37	69.20	3.61	38.17

of attribute-relevant and appearance information. **FDeID-Toolbox** provides the standardized infrastructure necessary to track progress and benchmark future methods under reproducible, consistent conditions.

5 Additional Features

5.1 Method Ensemble

A unique capability enabled by our unified interface is *method ensemble*, which systematically combines multiple FDeID methods to achieve privacy-utility-quality trade-offs unattainable by any single method. We explore three ensemble strategies, with results summarized in Table 5.

Sequential Ensemble. Methods are applied in a pipeline, where the output of one method becomes the input to the next. This is particularly effective for combining complementary approaches, *e.g.*, a generative method that alters facial structure followed by an adversarial method that adds perturbations to confuse residual identity features:

$$\mathbf{x}_{\text{deid}} = f_n \circ f_{n-1} \circ \dots \circ f_1(\mathbf{x}_{\text{orig}}), \quad (1)$$

where f_i denotes the i -th FDeID method. As shown in Table 5, CIAGAN→TI-DIM boosts privacy protection, raising PSR from 53.0% (CIAGAN alone) to 77.8% while reducing TAR from 7.15% to 3.00%. Meanwhile, k -Same-Select→TI-DIM improves utility preservation (*e.g.*, gender accuracy increases from 60.2% to 87.8%) at the cost of weaker privacy compared to k -Same-Select alone.

Parallel Ensemble with Fusion. Multiple methods process the input independently, and their outputs are combined via weighted blending:

$$\mathbf{x}_{\text{deid}} = \sum_{i=1}^n w_i \cdot f_i(\mathbf{x}_{\text{orig}}), \quad \text{where } \sum_{i=1}^n w_i = 1. \quad (2)$$

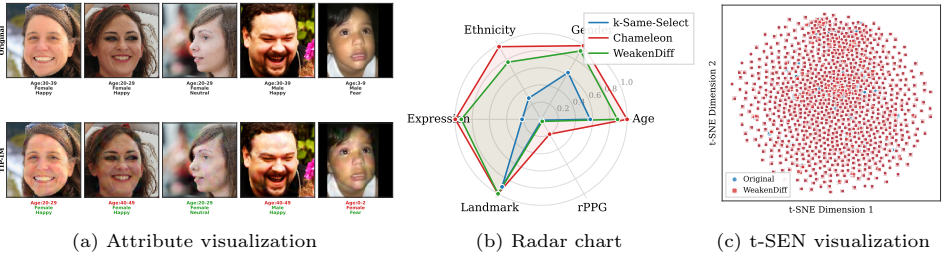


Fig. 4: Examples of the **FDeID-Toolbox**'s visualization module.

This strategy enables smooth interpolation between methods with complementary characteristics. Notably, $0.6 \times k\text{-Same-Select} + 0.4 \times \text{TI-DIM}$ achieves the highest PSNR of 38.82 dB among all ensemble configurations while also attaining strong utility (gender: 93.5%, expression: 68.3%), though at the expense of privacy (TAR rises to 97.8%). Conversely, $0.7 \times \text{CIAGAN} + 0.3 \times k\text{-Same-Select}$ maintains moderate privacy (TAR: 8.72%) with improved utility over either constituent method alone. **Attribute-Guided Ensemble.** Rather than manually selecting methods and weights, users specify which attributes to preserve or suppress, and the toolbox automatically configures an optimal ensemble based on per-method attribute preservation profiles from our benchmark. As shown in Table 5, all three attribute-guided configurations achieve consistently strong performance across metrics, with the `preserve={age, rPPG}` variant obtaining the best expression accuracy (69.4%) while maintaining high privacy (TAR: 90.3%). Compared to manual parallel fusion, attribute-guided ensembles deliver more balanced trade-offs without requiring domain expertise to tune individual method weights, substantially lowering the barrier to deploying effective de-identification pipelines.

5.2 Video Processing Pipeline

Beyond image-based evaluation, **FDeID-Toolbox** provides a video processing pipeline that supports both video files and frame-sequence directories through a unified input abstraction. The pipeline follows a detect-then-deidentify paradigm: RetinaFace [50] detects faces in each frame, and a selected method is applied to the detected face regions before reinsertion into the original frame. To enable real-time processing, we introduce a detection skipping strategy, which reuses bounding boxes from prior detections on intermediate frames, trading marginal spatial accuracy for substantial speedup.

5.3 Visualization and Analysis Tools

To support qualitative analysis, we provide a suite of visualization functions (as shown in Figure 4): (1) *side-by-side comparison* generates grid visualizations comparing multiple methods on the same input; (2) *attribute overlay* visualizes predicted attributes (age, gender, expression) on both original and de-identified

faces to diagnose utility degradation; (3) *metric radar charts* provide intuitive multi-dimensional comparison of methods across utilities; and (4) *identity embedding visualization* projects face embeddings into 2D space using t-SNE [62] to show identity separation between original and de-identified faces.

6 Conclusion

We present **FDeID-Toolbox**, a comprehensive and open-source for FDeID that addresses the longstanding challenges of fragmented implementations, inconsistent evaluation protocols, and incomparable results across studies. Our toolbox integrates 17 representative methods spanning four paradigms within a unified framework comprising modular data, method, pipeline, and evaluation components. Through benchmarking on mainstream datasets, we provide the systematic comparison across three evaluation dimensions: privacy protection, utility preservation, and visual quality. Our experiments reveal that no single method dominates all dimensions. We will release the codebase to facilitate reproducible research and accelerate progress in privacy-preserving computer vision.

Limitations. Despite the breadth of our toolbox, several limitations remain. First, our current evaluation is restricted to static images and does not address temporal consistency or identity leakage across video frames. Second, the current fairness analysis across demographic subgroups is limited, and a more thorough investigation of performance disparities with respect to age, gender, ethnicity, and skin tone is necessary to ensure equitable deployment of FDeID technologies.

Broader Impacts. FDeID is inherently dual-use, which can be misused to evade accountability or obstruct lawful identification. We encourage responsible use in compliance with applicable data protection regulations such as GDPR and urge practitioners to consider the ethical implications of their deployment contexts.

References

1. Hasan, M.R., Guest, R., Deravi, F.: Presentation-level privacy protection techniques for automated face recognition—a survey. *ACM Computing Surveys* **55**(13s) (2023) 1–27
2. Chow, K.H., Hu, S., Huang, T., Liu, L.: Personalized privacy protection mask against unauthorized facial recognition. In: *European Conference on Computer Vision*, Springer (2024) 434–450
3. He, X., Zhu, M., Chen, D., Wang, N., Gao, X.: Diff-privacy: Diffusion-based face privacy protection. *IEEE Transactions on Circuits and Systems for Video Technology* **34**(12) (2024) 13164–13176
4. Cai, Z., Gao, Z., Planche, B., Zheng, M., Chen, T., Asif, M.S., Wu, Z.: Disguise without disruption: Utility-preserving face de-identification. In: *Proceedings of the AAAI Conference on Artificial Intelligence*. Volume 38. (2024) 918–926
5. European Union: Regulation (eu) 2024/1689 of the european parliament and of the council of 13 june 2024 laying down harmonised rules on artificial intelligence. Official

- Journal of the European Union **L(2024/1689)** (2024) Entered into force: 2 August 2024.
6. U.S. Department of Health and Human Services: Standards for privacy of individually identifiable health information. 45 C.F.R. Parts 160 and 164 (2003)
 7. Newton, E.M., Sweeney, L., Malin, B.: Preserving privacy by de-identifying face images. *IEEE Transactions on Knowledge and Data Engineering* **17(2)** (2005) 232–243
 8. Gross, R., Sweeney, L., De la Torre, F., Baker, S.: Model-based face de-identification. In: *Proceedings of the IEEE/CVF Conference on Computer Vision and Pattern Recognition Workshop*, IEEE (2006) 161–161
 9. Du, L., Yi, M., Blasch, E., Ling, H.: Garp-face: Balancing privacy protection and utility preservation in face de-identification. In: *IEEE International Joint Conference on Biometrics*, IEEE (2014) 1–8
 10. Hukkelås, H., Mester, R., Lindseth, F.: Deepprivacy: A generative adversarial network for face anonymization. In: *International Symposium on Visual Computing*, Springer (2019) 565–578
 11. Cao, J., Liu, B., Wen, Y., Xie, R., Song, L.: Personalized and invertible face de-identification by disentangled identity information manipulation. In: *Proceedings of the IEEE/CVF International Conference on Computer Vision*. (2021) 3334–3342
 12. Hudson, S.E., Smith, I.: Techniques for addressing fundamental privacy and disruption tradeoffs in awareness support systems. In: *Proceedings of the ACM Conference on Computer Supported Cooperative Work*. (1996) 248–257
 13. Boyle, M., Edwards, C., Greenberg, S.: The effects of filtered video on awareness and privacy. In: *Proceedings of the 2000 ACM Conference on Computer Supported Cooperative Work*. (2000) 1–10
 14. Sweeney, L.: k-anonymity: A model for protecting privacy. *International journal of Uncertainty, Fuzziness and Knowledge-based Systems* **10(05)** (2002) 557–570
 15. Dong, Y., Liao, F., Pang, T., Su, H., Zhu, J., Hu, X., Li, J.: Boosting adversarial attacks with momentum. In: *Proceedings of the IEEE/CVF Conference on Computer Vision and Pattern Recognition*. (2018) 9185–9193
 16. Yang, X., Dong, Y., Pang, T., Su, H., Zhu, J., Chen, Y., Xue, H.: Towards face encryption by generating adversarial identity masks. In: *Proceedings of the IEEE/CVF International Conference on Computer Vision*. (2021) 3897–3907
 17. Wu, Y., Yang, F., Xu, Y., Ling, H.: Privacy-protective-gan for privacy preserving face de-identification. *Journal of Computer Science and Technology* **34(1)** (2019) 47–60
 18. Park, J., Lee, S., Shaheryar, M., Jung, S.K.: Facial identity editing: Towards effective de-identification. In: *IEEE International Conference on Image Processing*, IEEE (2025) 1792–1797
 19. Gross, R., Sweeney, L., De La Torre, F., Baker, S.: Semi-supervised learning of multi-factor models for face de-identification. In: *Proceedings of the IEEE/CVF Conference on Computer Vision and Pattern Recognition*. (2008) 1–8
 20. Maximov, M., Elezi, I., Leal-Taixé, L.: Ciagan: Conditional identity anonymization generative adversarial networks. In: *Proceedings of the IEEE/CVF Conference on Computer Vision and Pattern Recognition*. (2020) 5447–5456
 21. Wen, Y., Liu, B., Cao, J., Xie, R., Song, L., Li, Z.: Identitymask: Deep motion flow guided reversible face video de-identification. *IEEE Transactions on Circuits and Systems for Video Technology* **32(12)** (2022) 8353–8367
 22. Wen, Y., Liu, B., Cao, J., Xie, R., Song, L.: Divide and conquer: a two-step method for high quality face de-identification with model explainability. In: *Proceedings of the IEEE/CVF International Conference on Computer Vision*. (2023) 5148–5157

23. Yang, S., Wang, W., Cheng, Y., Dong, J.: A systematical solution for face de-identification. In: Chinese Conference on Biometric Recognition, Springer (2021) 20–30
24. Zhai, L., Guo, Q., Xie, X., Ma, L., Wang, Y.E., Liu, Y.: A³gan: Attribute-aware anonymization networks for face de-identification. In: Proceedings of the ACM International Conference on Multimedia. (2022) 5303–5313
25. Savic, M., Zhao, G.: De-identification of facial videos while preserving remote physiological utility. In: BMVC, BMVA Press (2023) 1–14
26. Liu, Y., Cheng, K.H., Savic, M., Chen, H., Yu, Z., Zhao, G.: 3d face de-identification with preserving multi-facial attributes: A benchmark. IEEE TBIOM (2025) 1–14
27. Kung, H.W., Varanka, T., Saha, S., Sim, T., Sebe, N.: Face anonymization made simple. In: WACV, IEEE (2025) 1040–1050
28. Zhu, B., Zhang, C., Sui, Y., Li, L.: Facemotionpreserve: A generative approach for facial de-identification and medical information preservation. Scientific Reports **14**(1) (2024) 17275
29. Hukkelås, H., Lindseth, F.: Deepprivacy2: Towards realistic full-body anonymization. In: Proceedings of the IEEE/CVF Winter Conference on Applications of Computer Vision. (2023) 1329–1338
30. Drawitsch, M.: deface: Video anonymization by face detection. <https://github.com/ORB-HD/deface> (2020)
31. Gross, R., Airoldi, E., Malin, B., Sweeney, L.: Integrating utility into face de-identification. In: International Workshop on Privacy Enhancing Technologies, Springer (2005) 227–242
32. Meng, L., Sun, Z.: Face de-identification with perfect privacy protection. In: International Convention on Information and Communication Technology, Electronics and Microelectronics, IEEE (2014) 1234–1239
33. Shamshad, F., Naseer, M., Nandakumar, K.: Clip2protect: Protecting facial privacy using text-guided makeup via adversarial latent search. In: Proceedings of the IEEE/CVF Conference on Computer Vision and Pattern Recognition. (2023) 20595–20605
34. Jia, S., Yin, B., Yao, T., Ding, S., Shen, C., Yang, X., Ma, C.: Adv-attribute: Inconspicuous and transferable adversarial attack on face recognition. In Koyejo, S., Mohamed, S., Agarwal, A., Belgrave, D., Cho, K., Oh, A., eds.: Advances in Neural Information Processing Systems. Volume 35. (2022) 34136–34147
35. Zhang, Y., Fang, Y., Cao, Y., Wu, J.: Rbgan: Realistic-generation and balanced-utility gan for face de-identification. Image and Vision Computing **141** (2024) 104868
36. Yang, H., Xu, X., Xu, C., Zhang, H., Qin, J., Wang, Y., Heng, P.A., He, S.: G²face: High-fidelity reversible face anonymization via generative and geometric priors. IEEE Transactions on Information Forensics and Security **19** (2024) 8773–8785
37. Meden, B., Gonzalez-Hernandez, M., Peer, P., Štruc, V.: Face deidentification with controllable privacy protection. Image and Vision Computing **134** (2023) 104678
38. Karras, T., Aila, T., Laine, S., Lehtinen, J.: Progressive growing of gans for improved quality, stability, and variation. In: International Conference on Learning Representations. (2018) 1–12
39. Liu, Z., Luo, P., Wang, X., Tang, X.: Deep learning face attributes in the wild. In: Proceedings of the IEEE/CVF International Conference on Computer Vision. (2015) 3730–3738

40. Huang, G.B., Mattar, M., Berg, T., Learned-Miller, E.: Labeled faces in the wild: A database for studying face recognition in unconstrained environments. In: Workshop on faces in 'Real-Life' Images: detection, alignment, and recognition. (2008) 1–11
41. Moschoglou, S., Papaioannou, A., Sagonas, C., Deng, J., Kotsia, I., Zafeiriou, S.: Agedb: The first manually collected, in-the-wild age database. In: Proceedings of the IEEE/CVF Conference on Computer Vision and Pattern Recognition Workshop. (2017) 51–59
42. Karkkainen, K., Joo, J.: Fairface: Face attribute dataset for balanced race, gender, and age for bias measurement and mitigation. In: Proceedings of the IEEE/CVF Winter Conference on Applications of Computer Vision. (2021) 1548–1558
43. Mollahosseini, A., Hasani, B., Mahoor, M.H.: Affectnet: A database for facial expression, valence, and arousal computing in the wild. *IEEE Transactions on Affective Computing* **10**(1) (2017) 18–31
44. Stricker, R., Müller, S., Gross, H.M.: Non-contact video-based pulse rate measurement on a mobile service robot. In: IEEE International Symposium on Robot and Human Interactive Communication, IEEE (2014) 1056–1062
45. Madry, A., Makelov, A., Schmidt, L., Tsipras, D., Vladu, A.: Towards deep learning models resistant to adversarial attacks. In: International Conference on Learning Representations. (2018)
46. Dong, Y., Pang, T., Su, H., Zhu, J.: Evading defenses to transferable adversarial examples by translation-invariant attacks. In: Proceedings of the IEEE/CVF Conference on Computer Vision and Pattern Recognition. (2019) 4312–4321
47. Yin, B., Wang, W., Yao, T., Guo, J., Kong, Z., Ding, S., Li, J., Liu, C.: Adv-makeup: A new imperceptible and transferable attack on face recognition. In: Proceedings of the International Joint Conference on Artificial Intelligence. (2021) 1–7
48. Hu, S., Liu, X., Zhang, Y., Li, M., Zhang, L.Y., Jin, H., Wu, L.: Protecting facial privacy: Generating adversarial identity masks via style-robust makeup transfer. In: Proceedings of the IEEE/CVF Conference on Computer Vision and Pattern Recognition. (2022) 15014–15023
49. Salar, A., Liu, Q., Tian, Y., Zhao, G.: Enhancing facial privacy protection via weakening diffusion purification. In: Proceedings of the IEEE/CVF Conference on Computer Vision and Pattern Recognition. (2025) 8235–8244
50. Deng, J., Guo, J., Ververas, E., Kotsia, I., Zafeiriou, S.: Retinaface: Single-shot multi-level face localisation in the wild. In: Proceedings of the IEEE/CVF Conference on Computer Vision and Pattern Recognition. (2020) 5203–5212
51. Wang, Z., Bovik, A.C., Sheikh, H.R., Simoncelli, E.P.: Image quality assessment: From error visibility to structural similarity. *IEEE Transactions on Image Processing* **13**(4) (2004) 600–612
52. Zhang, R., Isola, P., Efros, A.A., Shechtman, E., Wang, O.: The unreasonable effectiveness of deep features as a perceptual metric. In: Proceedings of the IEEE/CVF Conference on Computer Vision and Pattern Recognition. (2018) 586–595
53. Heusel, M., Ramsauer, H., Unterthiner, T., Nessler, B., Hochreiter, S.: Gans trained by a two time-scale update rule converge to a local nash equilibrium. In: Advances in Neural Information Processing Systems. (2017) 815–823
54. Szegedy, C., Vanhoucke, V., Ioffe, S., Shlens, J., Wojna, Z.: Rethinking the inception architecture for computer vision. In: Proceedings of the IEEE/CVF Conference on Computer Vision and Pattern Recognition. (2016) 2818–2826
55. Mittal, A., Soundararajan, R., Bovik, A.C.: Making a “completely blind” image quality analyzer. *IEEE Signal Processing Letters* **20**(3) (2012) 209–212

56. Zheng, C., Mendieta, M., Chen, C.: Poster: A pyramid cross-fusion transformer network for facial expression recognition. In: Proceedings of the IEEE/CVF International Conference on Computer Vision. (2023) 3146–3155
57. Wang, J., Sun, K., Cheng, T., Jiang, B., Deng, C., Zhao, Y., Liu, D., Mu, Y., Tan, M., Wang, X., et al.: Deep high-resolution representation learning for visual recognition. *IEEE Transactions on Pattern Analysis and Machine Intelligence* **43**(10) (2020) 3349–3364
58. Joshi, J., Agaian, S.S., Cho, Y.: Factorizephys: Matrix factorization for multidimensional attention in remote physiological sensing. In: Advances in Neural Information Processing Systems. Volume 37., NeurIPS (2024)
59. Deng, J., Guo, J., Xue, N., Zafeiriou, S.: Arcface: Additive angular margin loss for deep face recognition. In: Proceedings of the IEEE/CVF Conference on Computer Vision and Pattern Recognition. (2019) 4690–4699
60. Wang, H., Wang, Y., Zhou, Z., Ji, X., Gong, D., Zhou, J., Li, Z., Liu, W.: Cosface: Large margin cosine loss for deep face recognition. In: Proceedings of the IEEE/CVF Conference on Computer Vision and Pattern Recognition. (2018) 5265–5274
61. Kim, M., Jain, A.K., Liu, X.: Adaface: Quality adaptive margin for face recognition. In: Proceedings of the IEEE/CVF Conference on Computer Vision and Pattern Recognition. (2022) 18750–18759
62. Maaten, L.v.d., Hinton, G.: Visualizing data using t-sne. *Journal of Machine Learning Research* **9**(Nov) (2008) 2579–2605
63. Kazemi, V., Sullivan, J.: One millisecond face alignment with an ensemble of regression trees. In: Proceedings of the IEEE/CVF Conference on Computer Vision and Pattern Recognition. (2014) 1867–1874

A Outline

This supplementary material provides more details of all face de-identification (FDeID) algorithms implemented in the **FDeID-Toolbox**. Section B shows additional qualitative results. Section C describes the overall design and the pretrained dependency models. Section D details the three naive FDeID methods: Gaussian blur, pixelation, and masking. Section E presents the k -same family: k -Same-Average [7], k -Same-Select [31], and k -Same-Furthest [32]. Section F describes the adversarial perturbation methods: PGD [45], MI-FGSM [15], TI-DIM [46], TIP-IM [16], and Chameleon [2]. Section G covers the generative methods: CIA-GAN [20], AMT-GAN [48], Adv-Makeup [47], WeakenDiff [49], DeID-rPPG [25], and G²Face [36].

B Additional Qualitative Results

Figures 5 and 6 present comparisons of all 17 FDeID methods implemented in the **FDeID-Toolbox** across two face images drawn from the LFW [40] and AgeDB [41] dataset, respectively. Each image is organized by paradigm: naive, k -same-based, adversarial, and generative.

C FDeID-Toolbox Details

C.1 Codebase Overview

1. **Data Module** (`core/data/`): Unified data loaders and preprocessing pipelines for diverse face datasets with standardized annotation formats.
2. **Method Module** (`core/fdeid/`): De-identification algorithms spanning naive, k -same, adversarial, and generative paradigms.
3. **Ensemble Module** (`core/ensemble/`): Sequential, parallel, and attribute-guided method combination strategies.
4. **Evaluation Module** (`core/eval/`, `core/identity/`, `core/utility/`): Privacy, utility, and quality metrics with pretrained model backends.
5. **Visualization Module** (`core/visualization/`): Publication-quality figure generation including side-by-side comparisons, radar charts, t-SNE embedding plots, and attribute overlays.

C.2 Dependency Models

The **FDeID-Toolbox** relies on several pretrained models that serve as building blocks across the de-identification pipeline and evaluation framework. These models can be categorized into three groups: face detection, face recognition, and utility attribute prediction.

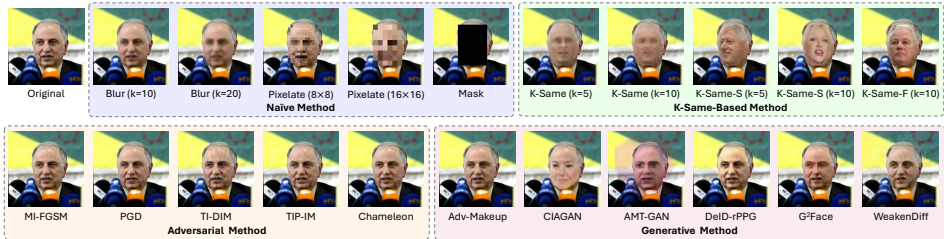


Fig. 5: **Qualitative comparison of FDeID methods on a sample face image.** The source image is from LFW dataset [40]. Methods are grouped by paradigm: naive, k -same-based, adversarial, and generative.



Fig. 6: **Qualitative comparison of FDeID methods on a sample face image.** The source image is from AgeDB dataset [41].

Face Detection. **RetinaFace** [50] is used as the primary face detector throughout the toolbox. It is based on a single-stage anchor-based detection framework and supports two backbone configurations: ResNet-50 and MobileNet-0.25. RetinaFace outputs bounding boxes with confidence scores and 5-point facial landmarks (left eye, right eye, nose tip, left mouth corner, right mouth corner), which are subsequently used for face alignment. Additionally, **Dlib** [63] is employed for 68-point facial landmark detection, which is required by several generative methods (*e.g.*, CIAGAN, AMT-GAN, Adv-Makeup) for precise face alignment and region-specific processing.

Face Recognition. Three face recognition models are integrated for both adversarial attack targets and privacy evaluation:

- **ArcFace** [59]: Uses a ResNet-100 backbone trained on MS1MV3 with additive angular margin loss. Produces 512-dimensional embeddings. It serves as the default surrogate model for all adversarial de-identification methods.
- **CosFace** [60]: Uses a ResNet-50 backbone trained on Glint360K with large-margin cosine loss. Produces 512-dimensional embeddings. It shares the same inference architecture as ArcFace but differs in the training loss formulation.
- **AdaFace** [61]: Employs an IR-SE backbone with adaptive margin based on image quality. Produces 512-dimensional embeddings. It includes built-in 5-point alignment utilities with a default crop size of 96×112 .

Table 6: Summary of dependency models used in the **FDeID-Toolbox** for face detection, recognition, and utility attribute evaluation.

Model	Task	Backbone	Input Size	Output
RetinaFace [50]	Face detection	ResNet-50	Variable	Bbox + 5 landmarks
Dlib [63]	Landmark detection	—	Variable	68 landmarks
ArcFace [59]	Face recognition	ResNet-100	112×112	512-d embedding
CosFace [60]	Face recognition	ResNet-50	112×112	512-d embedding
AdaFace [61]	Face recognition	IR-SE	112×112	512-d embedding
FairFace [42]	Age/Gender/Ethnicity	ResNet-34	224×224	18 classes
POSTER [56]	Expression	MobileFaceNet + IR-50	$112/224$	7 classes + 512-d
HRNet [57]	Landmarks	HRNet-W18	256×256	68×2 coords
FactorizePhys [58]	rPPG	3D CNN + NMF-FSAM	$72 \times 72 \times 160$	BVP signal

All three models are used to compute cosine similarity scores between original and de-identified face embeddings during privacy evaluation. The use of multiple recognition models provides a more robust privacy assessment, as different models may respond differently to de-identification artifacts.

Utility Attribute Prediction. Several pretrained models are employed for evaluating the preservation of semantic face attributes after de-identification:

- **FairFace** [42]: A ResNet-34 model trained for joint prediction of age (9 groups), gender (2 classes), and race/ethnicity (7 classes) with a unified 18-class output head. Input resolution: 224×224 . It is used for evaluating age, gender, and ethnicity preservation in our toolbox.
- **POSTER** [56]: A pyramid cross-fusion transformer for facial expression recognition. It employs a dual-backbone architecture: MobileFaceNet (112×112) for landmark-based geometric features and IR-50 (224×224) for appearance features, fused through a vision transformer (embed_dim=512, 8 heads). Classifies 7 basic expressions (neutral, happy, sad, surprise, fear, disgust, anger).
- **HRNet** [57]: High-Resolution Network for facial landmark detection. Maintains multi-scale representations through four parallel branches with repeated multi-scale fusion. Input: 256×256 ; output: 64×64 heatmaps for 68 landmark points. The Normalized Mean Error (NME) between original and de-identified landmarks quantifies geometric preservation.
- **FactorizePhys** [58]: A 3D CNN with factorized self-attention via non-negative matrix factorization for remote photoplethysmography (rPPG). Processes 160-frame video chunks at 72×72 resolution and extracts blood volume pulse (BVP) signals for non-contact heart rate estimation. Used to evaluate whether de-identification preserves the subtle color variations required for physiological signal extraction.

Table 6 summarizes all dependency models with their key specifications.

D Naive FDeID Methods

Naive methods apply classical image processing transformations to obscure facial identity. They are computationally efficient but generally offer limited utility preservation. The toolbox implements three naive methods in `core/fdeid/naive/`.

D.1 Gaussian Blur

Class: `GaussianBlurDeIdentifier`

Method name: `blur`

Gaussian blur applies a low-pass filter to the face region.

Parameters:

- `kernel_size` (int, default: 51): Gaussian kernel size (must be odd).
- `sigma` (float, default: 0): Gaussian sigma; 0 triggers automatic calculation based on kernel size.

D.2 Pixelation

Class: `PixelatedDeIdentifier`

Method name: `pixelate`

Pixelation creates a mosaic effect by downsampling and upsampling the face region.

Parameters:

- `block_size` (int, default: 16): Size of pixelation blocks.
- `interpolation` (str, default: `nearest`): Upsampling interpolation (`nearest` or `linear`).

D.3 Mask

Class: `MaskDeIdentifier`

Method name: `mask`

Replaces the entire face region with a solid color, providing strong privacy at the cost of complete attribute loss.

Parameters:

- `mask_color` (tuple, default: (0, 0, 0)): RGB color for the mask.
- `mask_type` (str, default: `solid`): One of `solid`, `random_color`, `white`, `black`.

E k -Same FDeID Methods

The k -same family of methods [7] achieves k -anonymity by replacing each face with a synthetic face derived from k similar faces in a reference dataset. All k -same methods are implemented in `core/fdeid/ksame/methods.py` and use pixel-wise L_2 distance for similarity matching.

E.1 k -Same-Average

Class: `KSameAverage`

Method name: `average` [7]

Parameters:

- `k` (int, default: 10): Number of similar faces to average.
- `reference_dataset` (str): Path to reference face images directory.
- `face_detector` (object): Face detector for extracting face crops from reference images.

E.2 k -Same-Select

Class: `KSameSelect`

Method name: `select` [31]

Parameters:

- `k` (int, default: 10): Number of similar faces to consider.
- `selection_mode` (str): Selection strategy—`closest`, `furthest`, or `random`.
- `reference_dataset` (str): Path to reference dataset.

E.3 k -Same-Furthest

Class: `KSameFurthest`

Method name: `furthest` [32]

Parameters:

- `k` (int, default: 10): Number of similar candidates.
- `reference_dataset` (str): Path to reference dataset.

F Adversarial FDeID Methods

Adversarial methods generate perturbations that cause face recognition models to fail. All adversarial methods are implemented in `core/fdeid/adversarial/` and share the following design principles:

- Perturbations are applied *only* to the extracted face region.
- Optimization minimizes cosine similarity between original and perturbed face embeddings.
- A default ArcFace model (ResNet-100, 512-d embeddings) is automatically created if not provided.

F.1 PGD

Class: PGDeIdentifier

Method name: pgd [45]

Parameters:

- `epsilon` (float, default: 8/255): Maximum perturbation budget.
- `alpha` (float, default: 2/255): Step size per iteration.
- `num_iter` (int, default: 20): Number of PGD iterations.
- `norm` (str, default: `Linf`): Norm constraint (`Linf`, `L2`, `L1`).
- `targeted` (bool, default: `False`): Targeted *vs.* untargeted attack.
- `random_start` (bool, default: `True`): Random initialization within ϵ -ball.

F.2 MI-FGSM

Class: MIFGSMDeIdentifier

Method name: mifgsm [15]

Parameters:

- `epsilon` (float, default: 8/255): Perturbation budget.
- `alpha` (float, default: 2/255): Step size.
- `num_iter` (int, default: 20): Number of iterations.
- `decay_factor` (float, default: 1.0): Momentum accumulation factor μ .

F.3 TI-DIM

Class: TIDIMDeIdentifier

Method name: tidim [46]

Parameters:

- `epsilon` (float, default: 8/255): Perturbation budget.
- `alpha` (float, default: 2/255): Step size.
- `num_iter` (int, default: 20): Number of iterations.
- `decay_factor` (float, default: 1.0): Momentum factor.
- `kernel_size` (int, default: 15): Gaussian kernel size for translation invariance.
- `prob` (float, default: 0.7): Probability of applying diverse input transformation.

F.4 TIP-IM

Class: TIPIMDeIdentifier

Method name: tipim [16]

Parameters:

- `epsilon` (float, default: 16/255): Perturbation budget.
- `alpha` (float, default: 2/255): Step size.
- `num_iter` (int, default: 100): Number of iterations.
- `gamma` (float, default: 10.0): Perceptual loss weight.
- `decay_factor` (float, default: 1.0): Momentum factor.
- `kernel_size` (int, default: 15): Gaussian kernel size.
- `use_diverse_input` (bool, default: True): Enable diverse input transformation.

F.5 Chameleon

Class: `ChameleonDeIdentifier`

Method name: `chameleon` [2]

Parameters:

- `epsilon` (float, default: 16/255): Perturbation budget.
- `alpha` (float, default: 0.001): Learning rate.
- `num_iter` (int, default: 20): Number of iterations.
- `lambda_dsim` (float, default: 1.0): Initial dissimilarity constraint weight.

G Generative De-Identification Methods

Generative methods employ generative models, including GANs, autoencoders, and diffusion models, to synthesize de-identified faces. These methods generally achieve higher visual quality but require pretrained model weights. All generative methods are implemented in `core/fdeid/generative/`.

G.1 CIAGAN

Class: `CIAGANDeIdentifier`

Method name: `ciagan` [20]

Parameters:

- `weights_path`: Path to CIAGAN generator weights.
- `retinaface_path`: Path to RetinaFace detector weights.
- `dlib_path`: Path to Dlib landmark predictor.

G.2 AMT-GAN

Class: `AMTGANDeIdentifier`

Method name: `amtgan` [48]

Parameters:

- `weights_path`: Path to generator weights.
- `reference_path`: Path to a single reference makeup image.
- `reference_dir`: Directory with multiple reference images.
- `dlib_path`: Optional Dlib predictor for facial masking.

G.3 Adv-Makeup

Class: `AdvMakeupDeIdentifier`

Method name: `advmakeup` [47]

Parameters:

- `weights_path`: Path to encoder/decoder weights directory.
- `target_name` (str, default: 00288): Target identity style.
- `dlib_path`: Path to Dlib landmark predictor.

G.4 WeakenDiff

Class: `WeakenDiffDeIdentifier`

Method name: `weakendiff` [49]

Parameters and presets:

- `prot_steps`: Protection optimization steps.
- `diffusion_steps`: Number of diffusion iterations.
- `start_step`: Diffusion start step.
- `null_optimization_steps`: Null text optimization iterations.
- `adv_optim_weight`: Adversarial optimization weight.
- `preset` (str): Quality preset:
 - `fast`: steps=(10, 10, 5)
 - `balanced`: steps=(15, 15, 10)
 - `quality`: steps=(30, 20, 20)

G.5 DeID-rPPG

Class: `DeIDrPPGDeIdentifier`

Method name: `deid_rppg` [25]

Parameters:

- `chunk_size` (int, default: 64): Number of frames per chunk.
- `face_size` (int, default: 128): Face crop resolution.
- `overlap` (int, default: 0): Frame overlap between chunks.

G.6 G²Face

Class: G²FaceDeIdentifier

Method name: G²Face [36]

Parameters:

- `image_size` (int, default: 256): Input resolution.
- `weights_path`: Path to G²Face checkpoint.
- `arcface_path`: Path to ArcFace weights.
- `recon_path`: Path to 3D reconstruction model.